ERDC TN-SWWRP-06-7
June 2006

Cascade Version 1: Theory and Model Formulation

By Magnus Larson, Nicholas C. Kraus, and Kenneth J. Connell

PURPOSE: This technical note describes the physical processes background of the numerical model Cascade, Version 1, which simulates long-term, regional sediment transport and coastal evolution. Cascade can be applied to reaches of coast covering hundreds of kilometers at which morphologic evolution extending to centuries may be of interest. The setting may encompass several barrier islands separated by inlets at which sediment is transferred through tidal-shoal complexes and dredging. Cascade capabilities are demonstrated at two sites located on the United States east coast to illustrate typical applications. The first technical note in the Cascade series describes the Interface (Connell and Kraus 2006). Version 1 of Cascade mathematically describes longshore sediment processes, with cross-shore processes represented schematically. Research is underway to represent cross-shore processes at a basic level associated with, for example, storms and long-term forcing, such as wind and cliff erosion.

BACKGROUND: Many Federal coastal inlets have been in place for more than a century, and their range and type of morphologic influence can far exceed local project dimensions (Kraus 2006). Both stabilized inlets and natural inlets can alter longshore sediment-transport pathways for tens to hundreds of kilometers, and formation of ebb shoals and flood shoals at newly cut inlets removes sediment that would otherwise be available to the beaches. In the Cascade model, the sediment is assumed to consist primarily of sand. Sand placed on beaches as nourishment likewise will travel far beyond project limits. The time and space scales of coastal projects call for regional modeling to address the full consequences and interactions of engineering activities, as well as the wide-scale of influence of natural processes and features (Larson et al. 2002a). Quantitative descriptions of regional coastal sediment processes are lacking, and their consideration raises new and interesting questions, together with many challenges.

To address these issues, a new class of numerical model of longshore transport and coastal change called Cascade was developed to represent regional processes extending hundreds of kilometers and covering multiple coastal inlets (Larson et al. 2002b; Larson and Kraus 2003). Time intervals of interest span decades to centuries. At regional time and space scales, at process level Cascade Version 1 mathematically describes such phenomena as longshore sand transport, ebb- and flood-tidal shoal evolution, bypassing bars between beaches and inlets, regional trends in the shape of the coast, and response of the shoreline and longshore transport to shore-normal structures. In Version 1, primarily cross-shore processes such as wind-blown sand, modifications of beach morphology by storms, placement of periodic beach nourishment, and overwash are represented schematically (conditions and rates input by the user).

The name Cascade derives from recognition that processes at different spatial and temporal scales act simultaneously in what can be viewed as cascading of scales from regional to local. For example, offshore contours of a coastal region might have a curved trend, upon which local projects are emplaced (and interact) that may individually appear to have straight trends in shoreline position. Another example is the gradual evolution of tidal shoal volumes under daily influence of longshore sediment transport as a source. The embedding of local processes requires cascading of information from wide-area to local, from long-term to immediate, and from project to project site.

MODELING APPROACH AND ASSUMPTIONS: At regional scale, coastline shapes and features are often encountered that are difficult to reproduce and maintain by means of existing coastal evolution models. The governing equations tend to diffuse such features towards a straight line because of the gradients in the coastline orientation. In contrast, there are processes and controls at regional scale that shape the coastline, balancing the tendency for the transport relationship at the local scale to smooth out nearshore features. This observation suggests an approach to modeling coastal evolution at different scales with coupling between the processes at the various scales. In Cascade, a theory was formulated that provides this modeling framework, potentially allowing for an arbitrary number of scales. The coupling between coastal evolution at different scales is through a cascading process whereby the evolution at a certain scale provide background conditions for the evolution at the adjacent smaller scale.

In Cascade Version 1, the assumption is made that there are two scales, regional and local, at which the coast responds, represented by the shoreline position. Existing one-line models of shoreline change typically reproduce only the local scale response. The regional response would be associated with the large-scale shapes and features that are of interest to include in the present modeling, but which existing models tend to smooth. The forces for forming and maintaining shoreline shape at regional scale are large-scale gradients in the wave and current conditions, as well as various regional controls that might have wide-area variability alongshore, such as the offshore topography and changes in incident waves along the shore, as might be caused by land mass sheltering.

In summary, alongshore gradients in transport processes at the regional scale can maintain complicated shoreline shapes. Assuming that we know and can quantify these gradients, a model can be developed to include them in simulating coastal evolution at the local scale.

MODEL STRUCTURE: Figure 1 is a schematic of a typical coastal setting to which Cascade may be applied. It shows three barrier islands separated by inlets with and without jetties, where the sediment is transferred around an inlet through the inlet-shoal complex. Sediment sources and sinks are represented, such as cliff erosion and wind-blown sand. The shoreline of the barrier island chain displays a curved trend at the regional scale with local variations in between the inlets.

Initial Cascade development focused on formulating fast, reliable, and robust algorithms for calculating longshore distributions of breaking waves and sediment (principally sand) transport. Also necessary was implementation of realistic boundary conditions, which in some cases constitute complex submodels (e.g., jetty bypassing and inlet sediment transfer). In the

following, main model components are summarized, including: (a) governing equations, (b) breaking wave properties, (c) longshore sediment transport, (d) bypassing transport, (e) inlet sediment storage and transfer, (f) sources and sinks, and (g) regional shoreline shape. Some of these components required new theories to be developed, whereas other components were based on existing knowledge. The summary here mainly covers new developments needed for Cascade.

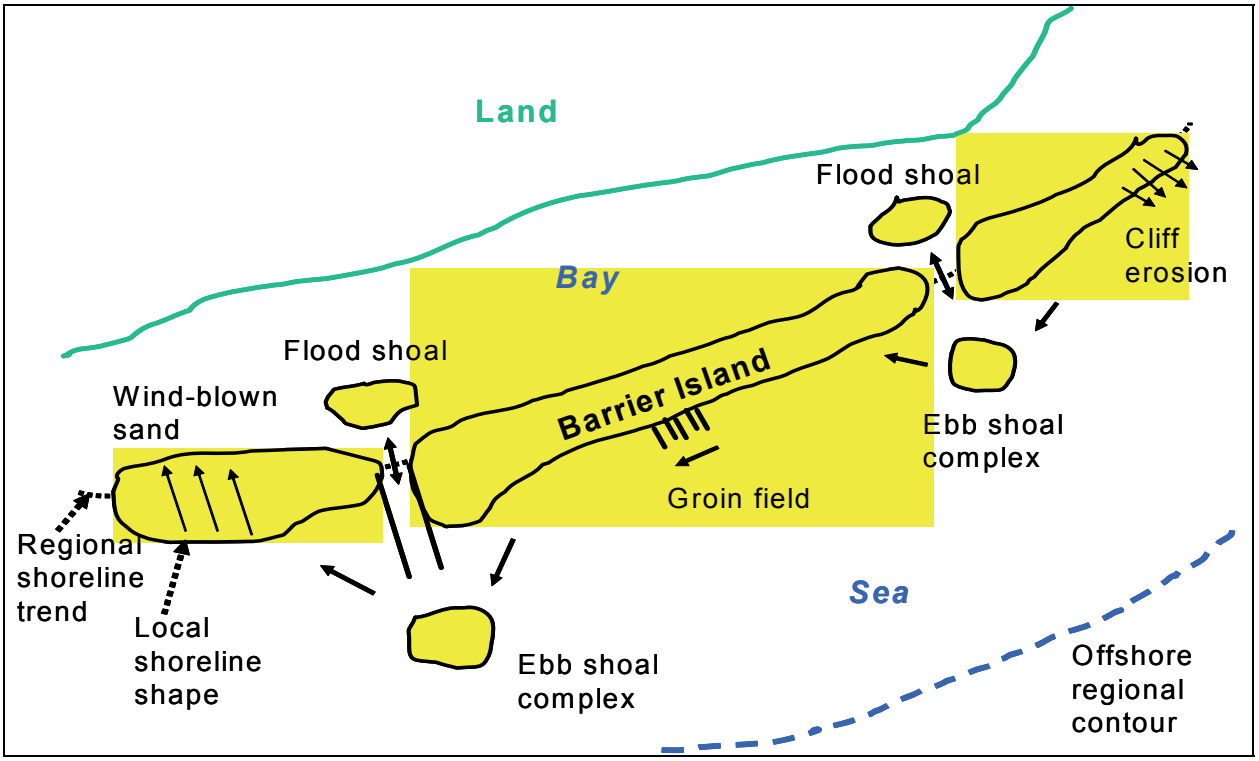

Figure 1. Overview of coastal setting to which Cascade model can be applied for simulating longshore sediment transport and coastal evolution

Governing Equations. In shoreline change modeling, which essentially corresponds to the local scale, the longshore sediment transport rate Q may be expressed as (Larson et al. 1987),

$$Q = Q_o \sin 2(\alpha_o) \tag{1}$$

where Q_o = transport rate amplitude (a function of the wave properties at breaking and the sediment characteristics), and α_o is the angle between the breaking waves and the local shoreline orientation expressed as,

$$\alpha_o = \alpha_b - \arctan(\partial y / \partial x) \tag{2}$$

where α_b = wave angle at breaking, y = shoreline position, and x = alongshore coordinate. If the regional transport rate is assumed to obey a similar relationship, then,

$$Q_r = Q_{or} \sin 2(\alpha_{or}) \tag{3}$$

$$\alpha_{or} = \alpha_{br} - \arctan(\partial y_r / \partial x) \tag{4}$$

in the same notation as with subscript *r* denoting the regional scale. The shoreline position y_r describes trends in the shoreline at the regional scale, being a function of the transport gradients at this scale.

In Cascade, it is assumed that the local shoreline evolves with respect to the regional shoreline, yielding the following transport equation:

$$Q = Q_o \sin 2\left(\alpha_b - \left(\arctan\left(\partial y / \partial x\right) - \arctan\left(\partial y_r / \partial x\right)\right)\right) \tag{5}$$

If y_r is in equilibrium (Q_r=0), as presently assumed in Cascade, Equation 4 implies that α_{br}=arctan(dy_r/dx). This relationship between α_{br} and y_r together with Equation 5, shows that the influence of the regional shoreline shape can be interpreted as an alongshore variation in the breaker angle superimposed on α_b. Thus, after the regional equilibrium shoreline shape y_r has been determined, y can be obtained directly by solving Equation 5 in combination with the sand volume conservation equation,

$$\frac{\partial Q}{\partial x} + D_T \frac{\partial y}{\partial t} = q(x,t) \tag{6}$$

where D_T = height of active profile (= D_C+D_B, where D_C is the depth of closure and D_B the berm height), t = time, and q = a source (sink) term varying in time, t, and alongshore.

Breaking Wave Properties. The transport rate Q must be calculated at a large number of points in space and for many time-steps. Thus, the wave properties at the breakpoint must be computed many times, and it is of great value to have an efficient algorithm to do this. Assuming input wave conditions in deep water, the wave properties at breaking are obtained by simultaneously solving the energy flux conservation equation and Snell's law, both equations taken from deep water to the breakpoint. The two equations are written as follows:

$$H_o^2 C_{go} \cos\theta_o = H_b^2 C_{gb} \cos\theta_b \tag{7}$$

$$\frac{\sin\theta_o}{C_o} = \frac{\sin\theta_b}{C_b} \tag{8}$$

where

H = wave height
C_g = group speed
C = phase speed
θ = wave angle ($= \alpha - \left(\arctan\left(\partial y / \partial x\right) - \arctan\left(\partial y_r / \partial x\right)\right)$)

and the subscripts *o* and *b* denote deep water and the breakpoint, respectively.

The two equations are coupled and are solved through an iterative procedure. Introducing expressions for the various wave quantities valid for deep and shallow water, and substituting the unknown angle from Snell's law into the energy flux conservation equation gives the following equation to solve with the water depth at breaking as the unknown,

$$\left(\frac{h_b}{L_o}\right)^{5/2} \cos\left(\arcsin\left(\sqrt{2\pi}\sin\theta_o\sqrt{\frac{h_b}{L_o}}\right)\right) = \left(\frac{H_o}{L_o}\right)^2 \frac{\cos\theta_o}{\gamma_b^2 2\sqrt{2\pi}} \tag{9}$$

where

h_b = water depth at the breakpoint
L_o = deepwater wavelength
γ_b = wave height to water depth at incipient depth-limited breaking (taken to be 0.78).

This equation shows that h_b/L_o (or, equivalently h_b/H_o) is a function only of H_o/L_o and θ_o. An empirical function was least-square fitted towards calculated data from Equation 9 so that h_b can be quickly obtained from known input wave properties. Once h_b is obtained, the other quantities at the breakpoint may be calculated directly. Figure 2 illustrates the variation of h_b/H_o with H_o/L_o and θ_o (solid lines).

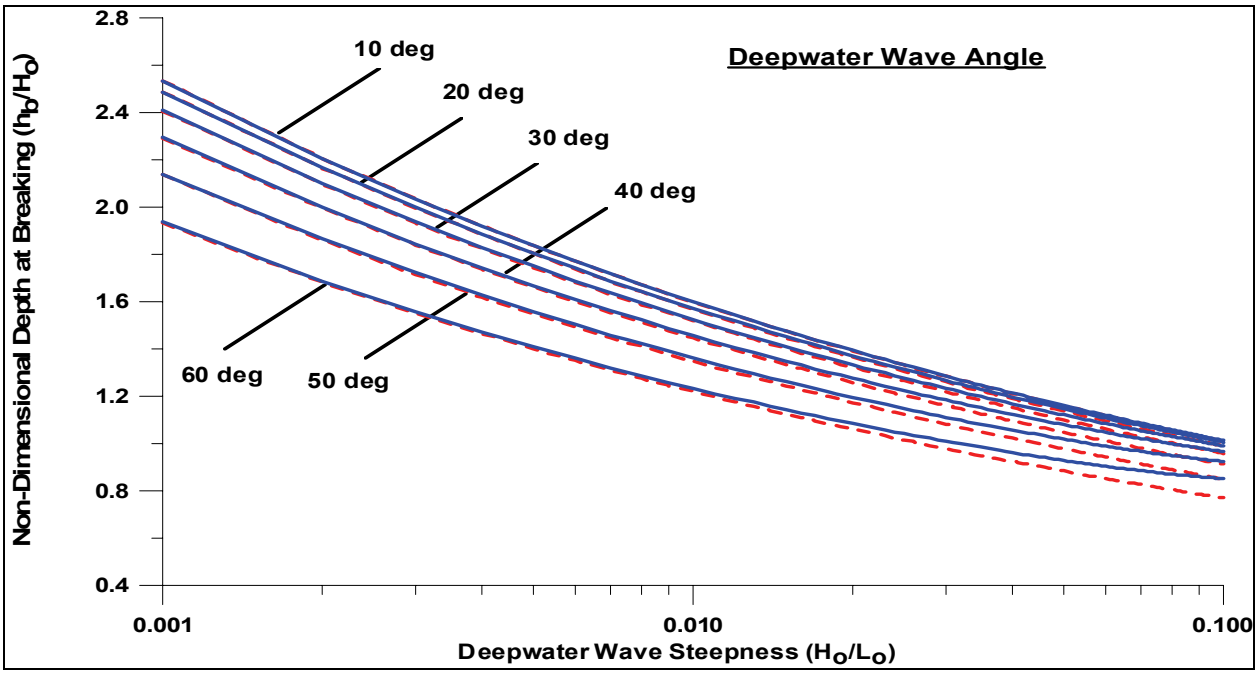

Figure 2. Normalized depth at breaking as a function of wave steepness and angle in deep water (exact and approximate solutions)

If the wave angle at breaking is small, $\cos\theta_b \cong 1.0$, Equation 9 simplifies, and h_b can be calculated explicitly from:

$$\frac{h_b}{L_o} = \left(\left(\frac{H_o}{L_o} \right)^2 \frac{\cos\theta_o}{\gamma_b^2 2\sqrt{2\pi}} \right)^{2/5} \tag{10}$$

Figure 2 also includes solutions for this approximate expression (broken lines), indicating that the error introduced by this expression is marginal for a wide range of values on H_o/L_o and θ_o (calculations showed that the error is maximum 10 percent for all wave angles and steepnesses). The wave angle at the breakpoint is calculated from Snell's law:

$$\theta_b = \arcsin\left(\sqrt{2\pi} \sin\theta_o \sqrt{\frac{h_b}{L_o}} \right) \tag{11}$$

Longshore Sediment Transport Rate. A recently derived formula (Larson and Hanson 1996; Larson and Bayram 2005) for the total longshore sediment transport rate is implemented in Cascade, in which it is possible to represent transport by currents generated by tide and wind, in addition to the current generated by obliquely incident breaking waves. In the derivation of this formula, it was assumed that suspended sediment mobilized by breaking waves is the dominant mode of transport in the surf zone.

A certain ratio of the incident wave energy flux provides the work for maintaining a steady-state concentration in the surf zone. The product between the concentration and the longshore current (from waves, wind, and tide) yields the transport rate Q as:

$$Q = \frac{\varepsilon}{(\rho_s - \rho)(1-a)gw} F\overline{V} \tag{12}$$

where

F = wave energy flux directed towards shore
$\overline{V}$ = surf-zone average longshore current velocity
ε = empirical coefficient, ρ_s (ρ)= sediment (water) density, a the porosity
w = sediment fall speed.

Hanson et al. (in preparation) and Bayram et al. (in preparation) showed that ε depends on the dimensionless fall speed evaluated at the breakpoint.

An alternative method for determining ε is to compare Equation 12 with the Coastal Engineering Research Center (CERC) formula. Larson and Bayram (2005) made such a comparison by calculating the mean longshore current in the surf zone based on the alongshore momentum equation with linearized friction and by computing F from linear wave theory. The Dean (1977, 1991) equilibrium beach profile ($h = Ax^{2/3}$) was assumed, in which the relationship between the shape parameter A and w is calculated from Kriebel et al. (1991). The transport coefficient is approximately given by $\varepsilon = 0.77 c_f K$, where K = transport rate coefficient in the CERC formula, and c_f = bottom friction coefficient, which is typically around 0.004-0.006 for field conditions

(Kraus and Larson 1991). At present, Cascade calculates ε from the input *K*-value by means of this relationship.

Bypassing at Jetties. To determine the bypassing at jetties (or groins), a model is needed to calculate the cross-shore distribution of the longshore transport rate updrift the jetty. Such a model was implemented in Cascade based on the sediment transport formula developed by Larson and Hanson (1996). This formula was derived under similar assumptions as the total longshore sediment transport formula previously discussed. However, because the local transport is needed, the concentration profile becomes a function of the local wave energy dissipation *P*. The transport rate per unit length across shore q_l is given by:

$$q_l = \frac{\varepsilon_c}{(\rho_s - \rho)(1-a)gw} VP \tag{13}$$

where V = local longshore current velocity, and ε_c = transport coefficient. The simplest approach to determine how much of the sediment that may bypass a groin or jetty is to assume that all sediment transported seaward of the groin tip is bypassed, whereas the transport shoreward of the tip is blocked.

To compute V and P, the random wave transformation model by Larson (1995) was employed, although a more simplified description of the energy dissipation due to breaking was used. Integrating q_l across the profile and assuming that the tip of the groin is located at $x = x_g$, the ratio p of the total sediment transport that bypasses the groin is:

$$p = \int_{x_g}^{\infty} \frac{1}{\sqrt{h}} \left(\frac{d\xi}{dx} \right)^2 dx \left\{ \int_0^{\infty} \frac{1}{\sqrt{h}} \left(\frac{d\xi}{dx} \right)^2 dx \right\}^{-1} \tag{14}$$

where ξ = ratio of breaking waves given by $\xi = \exp\left(-(\gamma_b h / H_x)^2\right)$, in which H_x = local root-mean-square (rms) wave height neglecting wave breaking.

Assuming an equilibrium beach profile, the bypass ratio p is a function of three nondimensional parameters and the incident wave angle, namely: $x_g/H_{rms,o}$, $H_{rms,o}/L_o$, $A/H_{rms,o}^{1/3}$, and θ_o. However, the dependence on refraction is weak for small wave angles at breaking. Figure 3 illustrates how the bypass ratio depends on normalized groin length and deepwater wave steepness for a fixed value on $A/H_{rms,o}^{1/3}$.

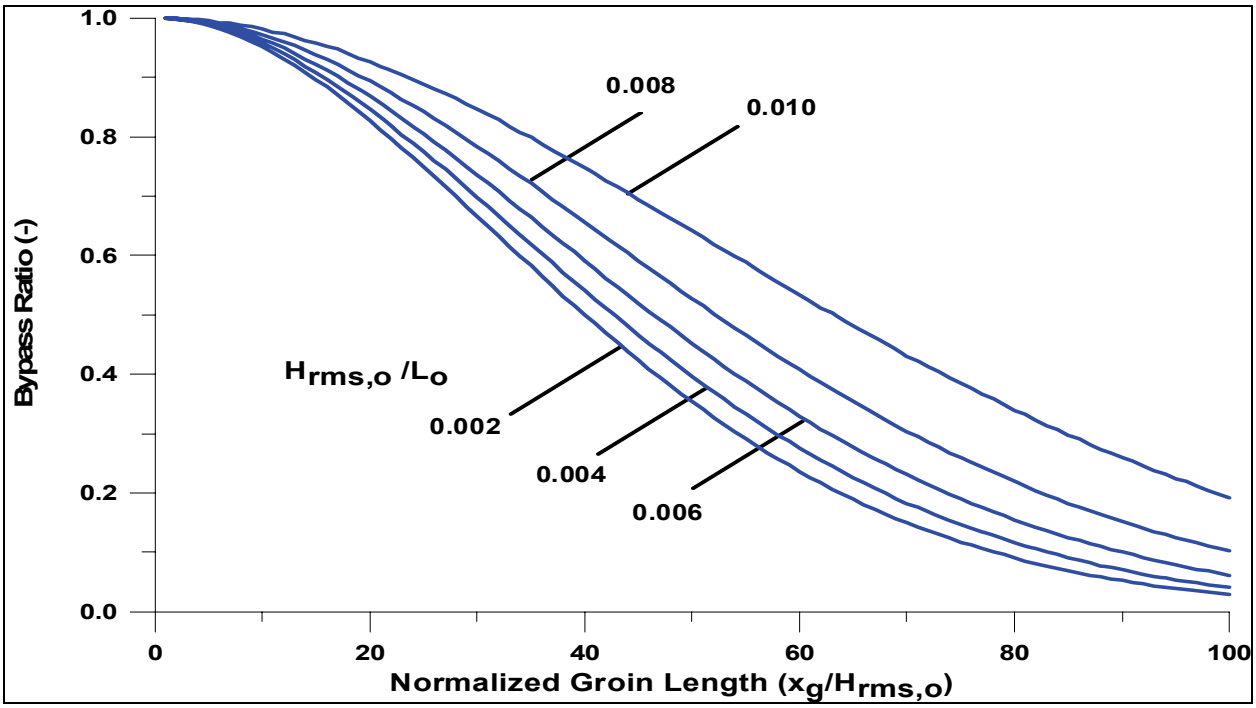

Figure 3. Bypass ratio as a function of normalized groin length and deepwater wave steepness for $A/H_{rms,o}^{1/3}$ = 0.1 (refraction neglected)

Inlet Sediment Storage and Transfer. Cascade incorporates the Inlet Reservoir Model (Kraus 2000) to describe sediment storage and transfer at coastal inlets. The inlet is schematized into distinct morphological units (ebb shoal proper, bypassing bars, and attachment bars) and relationships are formulated for how the sediment moves between them. Sediment that approaches the inlet and bypasses the jetty (determined by the bypassing ratio p) is transported to the ebb shoal. From the ebb shoal, the material is transferred to the bypassing bar and then further downdrift to the attachment bar. From the attachment bar, the sediment is transported along the shore. Each morphological unit is assumed to have a certain equilibrium volume for fixed hydrodynamic and sediment conditions. As the volumes approach equilibrium values, more sediment is transferred downdrift. Kraus (2000) assumed that the sediment passing through each unit is proportional to the ratio between the actual volume and the equilibrium volume for the unit. If equilibrium is attained, all sediment entering the particular morphologic unit is transferred downstream.

For each morphologic unit (ebb shoal, bypassing bar, attachment bar), two equations govern storage and transfer of sediment,

$$Q_{out} = Q_{in} \frac{W}{W_{eq}} \tag{15}$$

$$\frac{dW}{dt} = Q_{in} - Q_{out} \tag{16}$$

where

Q_{in} (Q_{out}) = transport to (from) the morphologic unit
W = sediment volume of the particular inlet morphologic unit
W_{eq} = its equilibrium volume

Walton and Adams (1976) derived empirical equations for the equilibrium shoal volume based on field data from 43 United States inlets approximately corresponding to the sum of the volumes of the ebb shoal proper and the bypassing bars. To employ these equations for computing W_{eq} of the different morphologic units, some assumptions must be made concerning the size relationship among them. Here, the assumption is made that the equilibrium volume ratio between the bypassing bar and the ebb shoal, as well as between the attachment bar and the ebb shoal, is constant. Presently, these ratios are set to 0.25 and 0.1, respectively. In the general case, transport can be directed both to the left and the right, and there will be bypassing and attachment bars on both sides of the inlet, that is, there will be five morphologic units. In the next version of Cascade, the inlet channel and flood shoal will be represented.

If the cross-sectional area of an inlet changes, it is necessary to allow for a time-varying $W_{Equation}$ During closure of an inlet, the W_{eq} that the tidal flow can maintain may fall below the actual volume in the ebb shoal complex, implying that sediment is released to adjacent beaches. Mathematically, Equations 15 and 16 can describe this situation, but from a physical point the release might be too rapid and cause unrealistic local growth of the shoreline. To remedy this situation, Equation 15 was changed into a nonlinear relationship according to $Q_{out}=Q_{in}(W/W_{eq})^n$, where n is a power. By specifying a value of $n < 1$ for situations where sediment is released to the beach, the release will be slower than for the linear model. For example, in simulations for Long Island, NY, n was set to 1.0 for periods when the ebb shoal complex was growing, whereas n = 0.1-0.2 best described the shoal experiencing a reduction in volume.

Sources and Sinks. In Cascade, sediment may be added or taken away from the coastal area through sources or sinks, respectively, creating a shoreline response. Common sediment sources are erosion of cliffs, bluffs, and dunes; beach nourishment, including placement of dredged material; wind-blown sand; river-transported sediment; and onshore transport of material from deeper water. Common sediment sinks are wind-blown sand; dredging; barrier-island wash-over; and offshore transport of material to deeper water. Thus, certain processes may act both as a source and a sink for the coast, depending on the particular conditions. In Version 1 of Cascade, an arbitrary number of sources and sinks may be specified having varying location in space and strength in time. Most of the transport related to sediment sources and sinks involves cross-shore processes. Future model development will focus on replacing the schematic source and sink descriptions with time-dependent process-based transport formulas related to the governing physical parameters.

Regional Shoreline Shape. In this section, guidance is given to determine the regional shoreline, and additional discussion is provided through two applications. If there is uncertainty in deriving the regional shoreline, it is recommended to simulate the evolution for different regional shoreline shapes to evaluate sensitivity and accuracy of results to the specified shape.

The regional coastal trend or regional shoreline shape is assumed constant and is an input quantity that is specified before simulations are performed. In the absence of a persistent locally induced disturbance, such as response of the shoreline to jetties, the shoreline will eventually evolve towards the regional shoreline, implying that the latter shoreline represents an equilibrium determined by constraints or processes acting at the regional level. For example, a single beach nourishment along an open coast will eventually be transported along the coast, and the shoreline will return to its pre-fill shape, whereas the placement of structure on a beach may induce a permanent disturbance of the regional shape. It may not be straightforward to define the regional shoreline, because often limited information is available on the undisturbed condition.

Referring to Equation 5, shoreline evolution is assumed to be the result of an alongshore variation in breaker angle given by $\alpha_{br}(x)+\alpha_b(x,t)$, where subtle variations in α_{br} maintain the regional trend. The breaker angle term α_b represents the contribution at the local scale obtained through a traditional refraction calculation from the offshore wave conditions. At equilibrium ($Q = 0$), $\alpha_s = \alpha_{br} + \alpha_b$, where α_s is the shoreline orientation, and a shoreline shape is obtained where the regional trend is overlaid by local fluctuations induced through variations in the breaking wave pattern and the internal and external boundary conditions. Interpreting this geometrically, $\alpha_s - \alpha_{br}$ represents the deviation of the shoreline from the regional trend and $\alpha_b - (\alpha_s - \alpha_{br})$ quantifies the local breaker angle with respect to this deviation. Thus, the shoreline locally evolves with respect to the orientation of the regional trend. For example, if the shoreline has a regional trend corresponding to a curve, this could be modeled with a traditional one-line model where the curved shoreline is discretized in a finite number of stretches, each having its own coordinate system taken along the trend of the shoreline for the particular stretch. Applying the formulation represents a similar approach, but in a continuous manner.

One approach for deriving the regional shoreline is through filtering of a measured regional shoreline for which the local disturbances are relatively small. The regional shoreline is then defined by:

$$y_r(x,t_m)=\frac{1}{\Delta s}\int_{x-\Delta s/2}^{x+\Delta s/2} y(x,t_m)dx \tag{17}$$

where

y_r = regional shoreline
Δs = an appropriately selected spatial window
y = shoreline position recorded at time t_m.

In this filtering approach, the main question is how to select Δs (discussed later in connection with the field applications).

BOUNDARY CONDITIONS AND NUMERICAL IMPLEMENTATION: At present, four boundary conditions (BC) have been formulated for use in Cascade:

a. No transport ($Q = 0$).

b. No shoreline change ($\partial Q/\partial x = 0$).

c. Bypassing ($Q = Q_b$).

d. Bypassing and inlet sediment storage and transfer.

The BCs may be specified as internal or external depending on whether they are located inside the grid or on the ends of the grid, respectively. Two external BCs are required (at grid cell boundaries number 1 and N+1, where N is the number of grid cells), and any number of internal BCs can be specified, as required in the particular application.

The first two BC types, total blockage of the longshore transport and no change in the shoreline position, are the ones commonly employed in shoreline modeling and are straightforward to implement. In Cascade, bypassing and inlet BC's constitutes submodels involving specifically developed algorithms. In the situation of bypassing of a jetty, the cross-shore distribution of the longshore sediment transport is first determined. The bypassing ratio is then obtained from the geometrical blockage of the transport distribution by the jetty. This ratio is applied to the calculated total longshore transport to estimate the transport that goes around the tip of the jetty. The bypassing algorithm also enters the inlet BC to compute the input transport to the ebb shoal. The Inlet Reservoir Model (Kraus 2000) then calculates the amount of sediment stored in the ebb shoal complex and the transfer of sediment to the downdrift side.

A staggered grid is employed to numerically solve the governing equations with Q-points (longshore transport rates) at the boundaries of the cells and y-points (shoreline position) in the middle of the cells. The equations are discretized in an explicit finite-difference solution method. Transport rates are calculated along the grid at time t, after which shoreline positions are updated at $t + \Delta t$ using the continuity equation, where Δt is the time-step. Both external and interal BC's are expressed in terms of Q.

The baseline for the grid should be oriented along the main trend of the regional shoreline. Because the shoreline is assumed to evolve locally with respect to the regional shoreline, if an inappropriate baseline is selected, the regional shoreline will have gradients that are large, which may degrade resolution of the calculations or create geometric conditions that are difficult to represent in the model.

CASCADE APPLICATIONS: Two field applications of Cascade are discussed that concern inlet opening and the associated coastal evolution. The first application involves the south shore of Long Island, NY, and the opening of Moriches Inlet and Shinnecock Inlet. The second application concerns the Delmarva Peninsula (involving the coasts of Delaware, Maryland, and Virginia) and the opening of Ocean City Inlet, MD. In the applications, simulated shoreline evolution and ebb shoal development are compared with measurements. The simulations cover time periods of about 50 years over a coastal extent of more than 100 km, where several different types of coastal processes and engineering activities enter, such as cliff erosion, overwash, beach nourishment, and shoreline response to jetties and groins.

Modeling Evolution of the Long Island South Shore. The eastern portion of the south shore of Long Island, NY (Figure 4), was selected for validating the capability of Cascade to simulate longshore sediment transport and coastal evolution on regional scale because several studies (e.g., Kana 1995; Bocamazo and Grosskopf 1999; Rosati et al. 1999) provide substantial

information for model validation. The stretch includes many coastal features and processes characterizing evolution on the regional scale. The study area extended from Fire Island Inlet to Montauk Point (hereafter referred to as FIMP) because most available information originates along this coastal stretch. The area includes Shinnecock Inlet and Moriches Inlet internal to the grid, and Fire Island Inlet as its western boundary. The channel cross-sectional areas of Moriches Inlet and Shinnecock Inlet have varied substantially with time, altering the size of the ebb shoal complexes and sediment removed from the nearshore transport system, providing an opportunity to model a complex morphologic system.

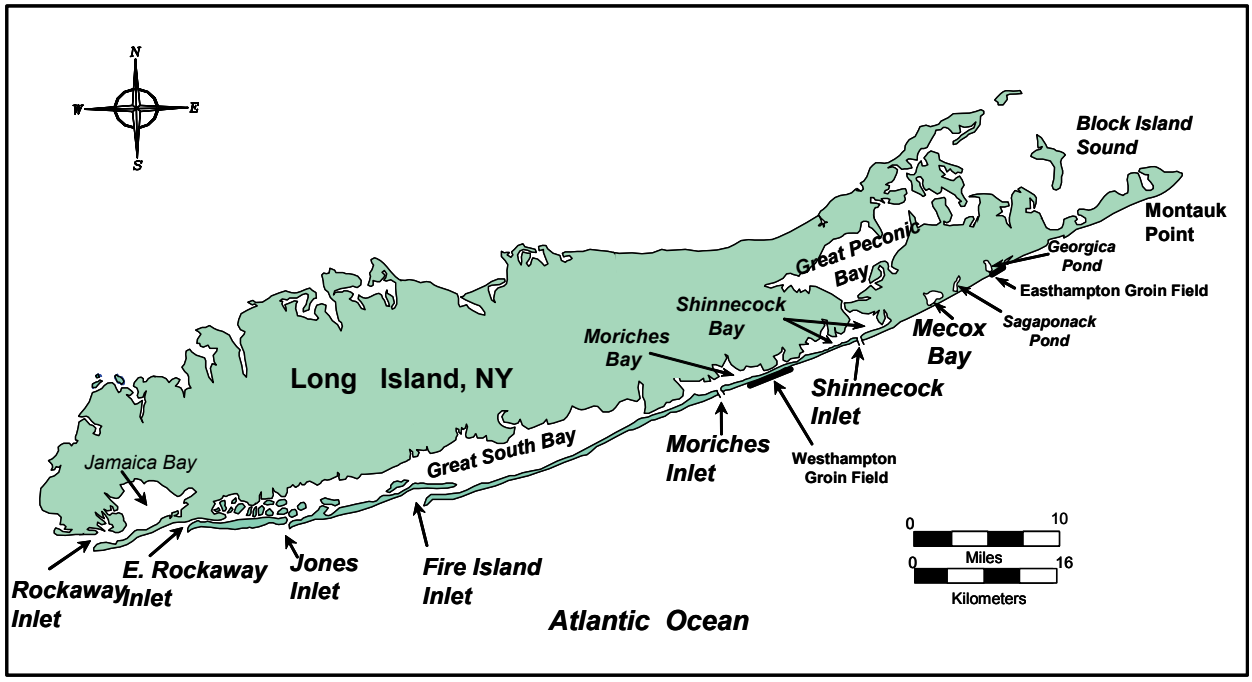

Figure 4. Location map for Fire Island to Montauk Point area, Long Island, NY

Two types of simulations were performed with Cascade for the FIMP area, that is, determining the overall annual net longshore transport pattern along the coast (based on shoreline positions and waves from 1983 to 1995), and simulating coastal evolution in connection with the opening of Moriches Inlet and Shinnecock Inlet (simulation period 1931-1983). Objectives of these simulations were to validate that the model could predict longshore sediment transport rates along a stretch of coastline where trends in the wave climate and shoreline shape are present at the regional scale, and predict coastal evolution in terms of shoreline response and changes in the ebb-shoal complex where regional processes and controls exert a significant influence on local processes.

General model setup. The south shore of Long Island is approximately oriented 67.5 deg True North, and a baseline was defined along that same orientation. In defining the baseline, locations employed by Rosati et al. (1999) were referenced. The lateral BC of "no shoreline change" was specified based on shoreline measurements covering 1830 to 1995. Suitable locations for such a BC were identified approximately 10 km west of Montauk Point and either adjacent to or 15 km east of Fire Island Inlet, depending on the simulation period. In simulation of inlet openings, the boundary was placed about 15 km east of Fire Island Inlet to avoid

describing spit movement taking place there. The time-step was set at 24 hr, and length step at 500 m.

The length of the modeled shoreline in combination with shadowing from continental landmasses and Long Island made it necessary to account for variation in wave climate alongshore. Hindcast waves from Wave Information Study (WIS)[1] stations 75, 78, and 81 were input (20-year time series of wave height, period, and angle from 1976 to 1995), linearly interpolated between stations. The height of active sediment transport was set to D_T = 8 m, and the representative median grain size was taken as 0.3 mm. The shoreline exhibits regional (large-scale) geomorphology that persists with time. Without taking these features into account through y_r, diffusion would eliminate them. In Cascade, y_r enters as a source term in the governing transport equation for the local shoreline evolution y. The shape of y_r was determined from spatial filtering of the shoreline measured in 1870, when Moriches Inlet and Shinnecock Inlet were not present, using a window length in Equation 17 of 7 km.

For the long-term simulation 1931-1983, the equilibrium volumes of the ebb shoals and bypassing bars were specified as a function of time based on the recorded inlet cross-sectional areas. In the shorter simulation 1983-1996, the equilibrium volumes were held constant because the inlets did not change substantially during this period. Jetty lengths on each side of the inlets and the time of construction were specified according to records. Two sources of sediment were included in the present Cascade simulations for the FIMP area as input from cliff erosion west of Montauk Point and from beach fills placed west of Shinnecock Inlet. A total fill volume of about 800,000 m^3 was placed west of Shinnecock Inlet between 1949 and 1983, and another 1,150,000 m^3 was placed in this area between 1983 and 1995 (Morang 1999). Smaller beach fills have been placed at other locations, but were neglected. In the simulations, the beach fill volumes were converted to sediment sources with constant strength in time and space. Rosati et al. (1999) estimated the cliff erosion at Montauk Point to yield about 33,000 m^3/year, which was introduced as a distributed source with constant strength in time. The Westhampton groin field (Nersesian et al. 1992; Kraus et al. 1994; Bocamazo and Grosskopf 1999) was not resolved in the simulations.

Annual net longshore transport. Simulations were first carried out to reproduce annual net sand transport rates observed along the FIMP coast. The simulation period 1983 - 1995 was selected because hindcast waves and measured shorelines were available covering that period. The simulation involved calibration of the model where the value of the transport coefficient K was determined based on the agreement with available information on the annual net transport rate. This information derives mainly from sediment budget studies for the south shore of Long Island (Kana 1995; Rosati et al. 1999). Based on trial simulations, the value on transport coefficient was selected to K = 0.12, which is about a third of the recommended value for the CERC formula (K = 0.39, for significant wave height). This value on K produced calculated rates that agreed well with trends and values reported in the most recent literature (Rosati et al. 1999). The estimated ebb shoal equilibrium volume for Shinnecock Inlet was about 8 million m^3, and for Moriches Inlet it was 6 million m^3. Corresponding initial volumes in 1983 were determined to be approximately 3.5 and 4.9 million m^3 (Morang 1999), respectively.

[1] http://chl.erdc.usace.army.mil/CHL.aspx?p=s&a=Projects;147

Figure 5 plots the calculated annual net longshore transport rates compared with the rates estimated in the sediment budget study by Rosati et al. (1999). The calculated transport rates display expected regional behavior of increasing rates going west (Panuzio 1968), with a near-zero rate near Montauk Point. Estimates of transport rates from the sediment budget included in Figure 5 encompass the most likely value as well as an interval over which the rate could vary. The figure shows marked disturbances of the inlets on the transport pattern. Because both Shinnecock Inlet and Moriches Inlet act as sediment sinks, the calculated transport rates drop substantially around the inlets. The derived rates confirm this behavior, although they are somewhat less than the calculated ones at Moriches Inlet.

Coastal evolution in connection with inlet openings. The second simulation for Long Island, 1931-1983, covers the period when Moriches Inlet and Shinnecock Inlet were opened by hurricanes. The inlets subsequently experienced great changes in cross-sectional areas, and Moriches Inlet closed temporarily in 1951 before it was artificially opened. Figure 6 illustrates how the minimum cross-sectional area varied for the two inlets during the simulation period. The figure is based on information in Czerniak (1977) and Morang (1999), linearly interpolated to supply time-varying input values. Equilibrium shoal volumes were derived from the cross-sectional areas through an empirical relation (Walton and Adams 1976). It was assumed that the shoal and bars at the inlets would move towards equilibrium volumes defined based on the instantaneous cross-sectional areas. The same wave time series served as input as for the calculations of the annual net longshore sediment transport rate previously described. The three WIS stations provided wave information, and the time series derived for 1976-1995 was applied repetitively.

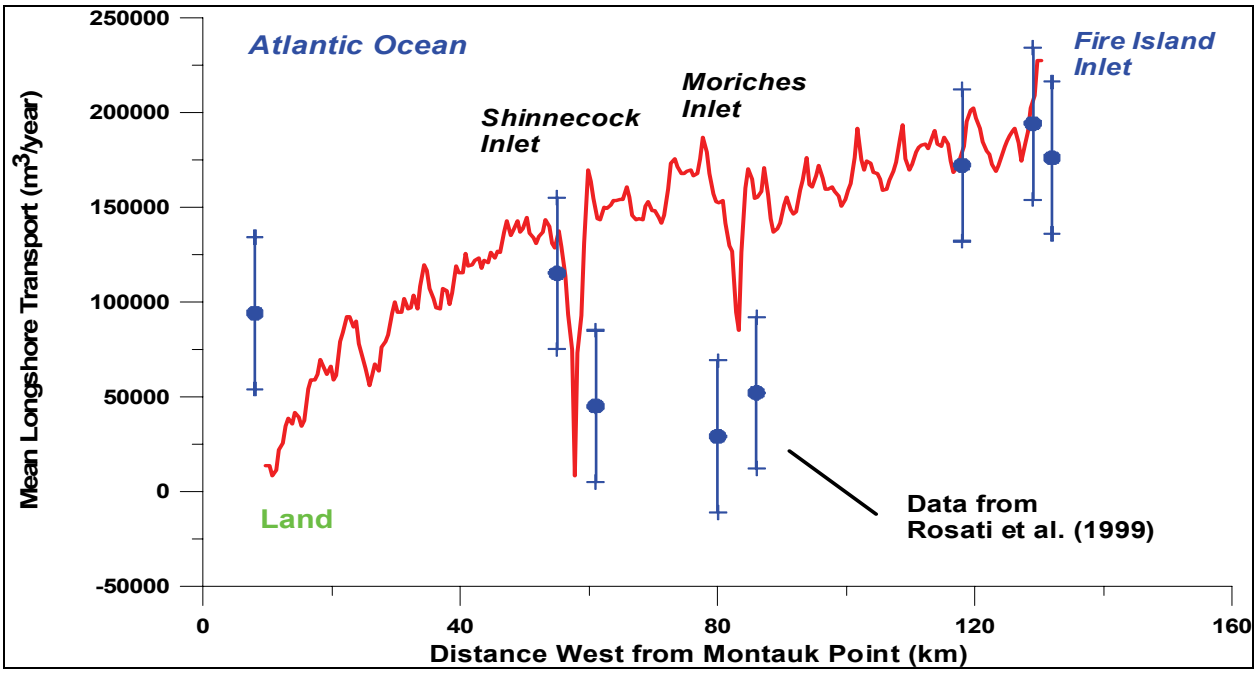

Figure 5. Calculated annual net transport rates along FIMP area based on wave data from 1983-95 compared with transport rates derived from sediment budget studies

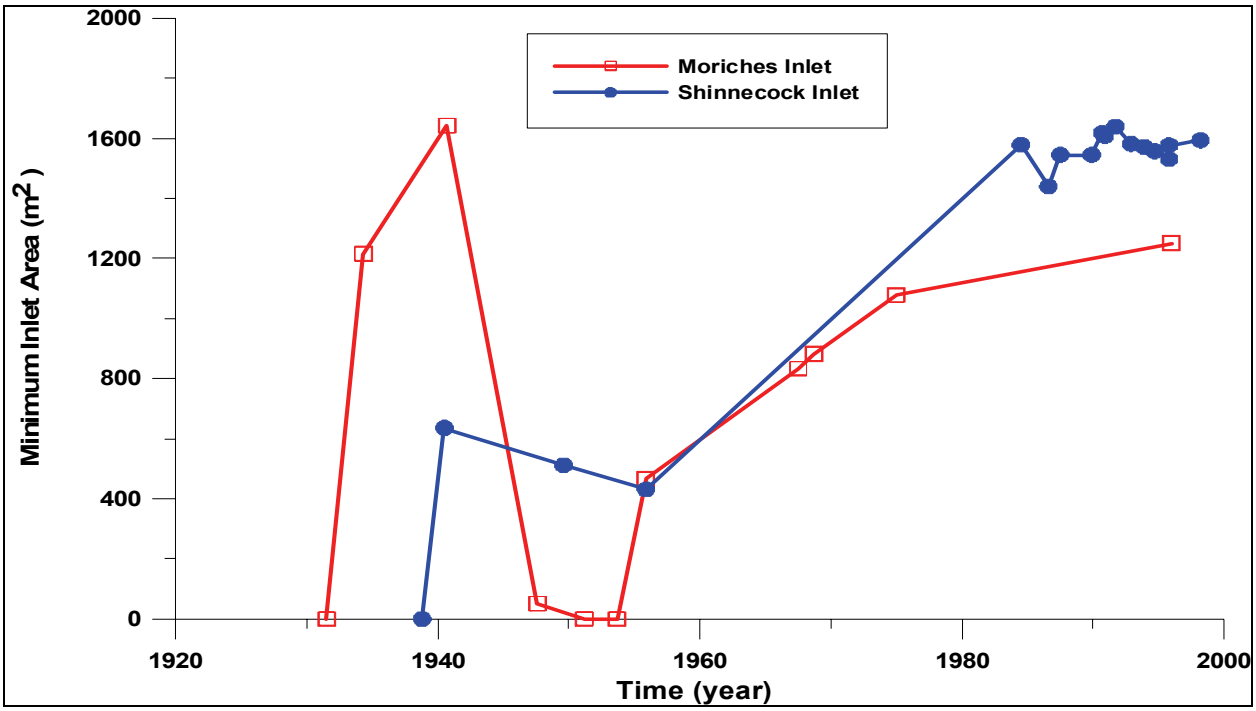

Figure 6. Time evolution of minimum inlet cross-sectional area for Moriches and Shinnecock Inlets based on Czerniak (1977) and Morang (1999)

Figure 7a plots measured and predicted shoreline positions in 1983 as well as the initial shoreline. The shoreline measured in 1870 was taken as the initial shoreline, because no measurements were available closer in time to 1931. The calculations yielded the correct magnitude of advance updrift and recession downdrift of the inlets, as well as the regional trend of shoreline evolution. Directly downdrift of the inlets, the predicted shoreline shape deviates somewhat from the measurements, attributed to incomplete representation of the influence of the attachment bar and tidal-induced transport near the inlet. Figure 7b displays an enlargement of the shorelines given in Figure 7a in the vicinity of the inlets.

Only limited data on the ebb shoal complex evolution were available, mostly for times after the end of the simulation period. However, these data still gave some indications on how well the model predicted the shoal and bar developments. A highly variable evolution was obtained for Moriches Inlet due to its history of opening and closing. Because of the small value of the exponent in the nonlinear reservoir model during the closing phase, the ebb shoal complex at Moriches Inlet did not release all of its sediment back to the beach even though the inlet remained closed for some period of time. The inlet submodel reproduced the essential features of the inlet behavior, as well as quantitatively predicting the growth of the shoals and bars, also for the case of a variable cross-sectional area.

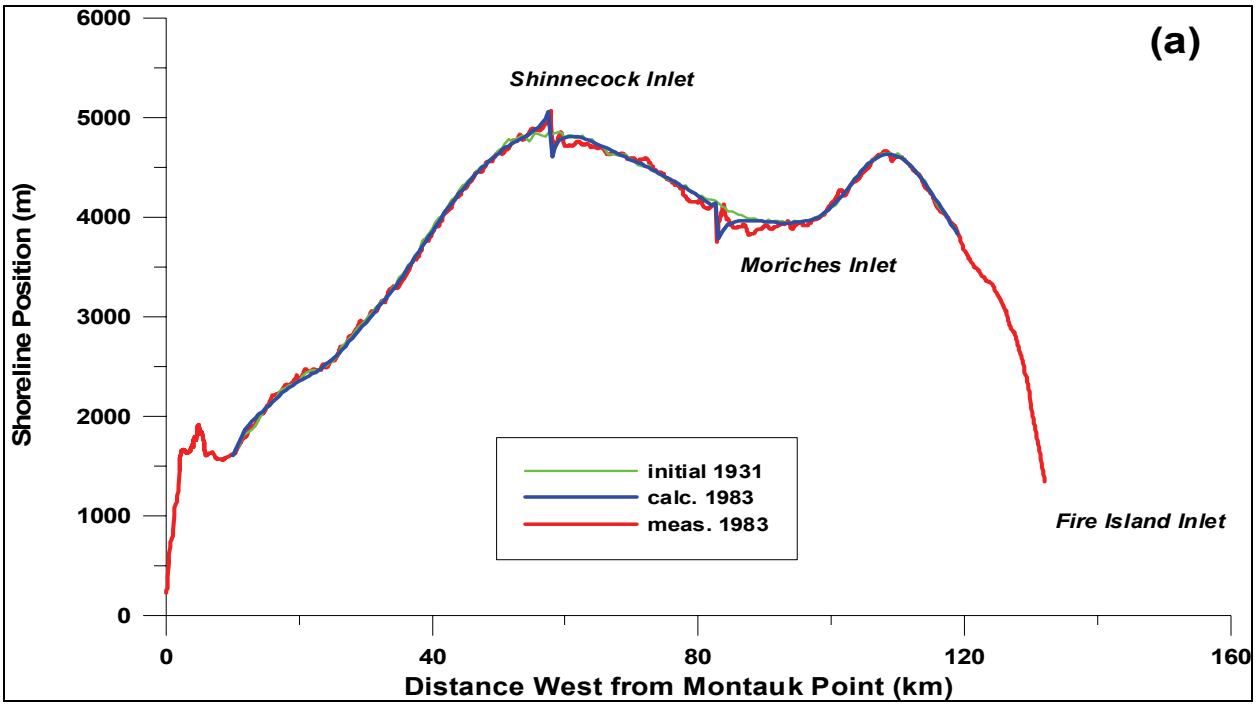

a. Overview

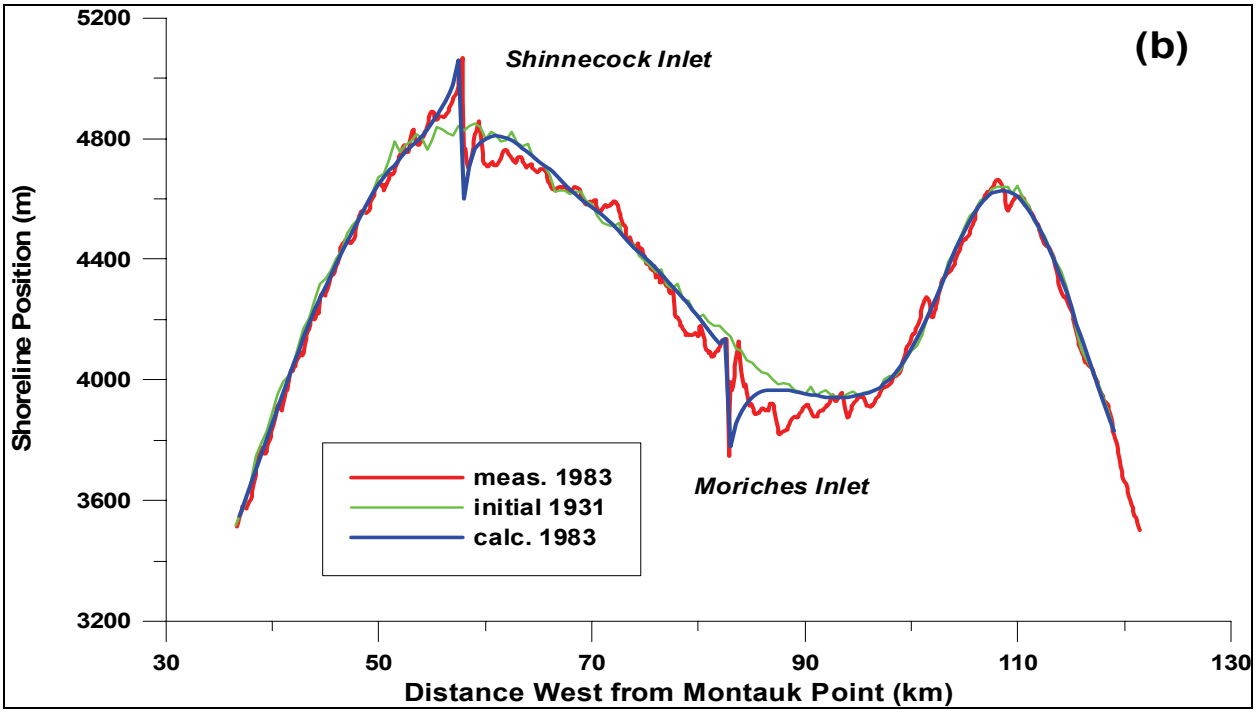

b. Detail

Figure 7. Comparison between simulated and measured shoreline 1983 together with initial shoreline

Modeling Evolution along Delmarva Peninsula. The Atlantic Ocean coast of Delaware, Maryland, and Virginia, part of the Delmarva Peninsula, covers approximately 100 km of barrier islands influenced by human alterations and development. Indian River Inlet, Delaware, and Ocean City Inlet, Maryland, have trapped significant sediment volumes in their ebb- and flood-tidal shoals (Figure 8). Engineering studies have been conducted for specific (local) sites (e.g., Dean and Perlin 1977; Lanan and Dalrymple 1977; Gebert et al. 1992; Stauble et al. 1993), but no quantitative regional studies are known.

Engineering actions in this area would benefit from availability of a predictive tool to address societal and environmental needs to bypass sediment at the inlets, design beach fills, adaptively manage erosional hot spots associated with the beach fill along Ocean City, regulate overwash along Assateague Island, and in general to understand the long-term evolution of the coast that extends from Cape Henlopen to the north to Chincoteague Inlet to the south. This coast exhibits several geomorphic features associated with the regional pattern of longshore sediment transport, including a nodal point in net transport between Indian River Inlet and Ocean City Inlet, large-scale curvature in the shoreline, prominent ebb-shoal development at the inlets, overwash on Assateague Island, and spit progradation at both the northern and southern ends of the reach.

General model setup. For the modeling, a coordinate system was defined with the x-axis (baseline) oriented along the main trend of the Delmarva Peninsula and the y-axis pointing offshore, with the origin located at the northern most point of the study area (at Cape Henlopen). The main simulation interval involved opening of Ocean City Inlet and encompassed the time period from 1933 to 1980. A time-step of 24 hr was specified for the simulations, and the grid covered a length of close to 90 km with a cell size of 500 m. The boundaries were placed about 10 km away from the spits at Cape Henlopen and Chincoteague, and the specified conditions at both boundaries were no change in shoreline location. Wave information from five WIS stations was the driving input, namely stations 62, 63, 64, 65, and 66, covering the 20-year hindcast period 1976-1995. Thus, for the long simulation interval, the wave input was permutated to yield the necessary number of input waves.

Measurements of the median grain size along the Delmarva Peninsula (Anders et al. 1987; Anders and Hansen 1990; Ramsey 1999) showed that the grain size is fairly constant north of Indian River Inlet, but decreases southward towards the state line between Delaware and Maryland. Based on these observations, the *K*-value in the CERC formula (referring to significant wave height) was set to 0.17 north of Indian River Inlet and then specified to grow linearly to 0.35 at the Delaware/Maryland state line, after which it was kept constant throughout the rest of the grid. For the northern part of the study area, half the recommended value of 0.39 (HQUSACE 2001; *Shore Protection Manual* 1984) was used, whereas for the southern part the value agreed with the standard value. It is expected that in modeling large areas on the regional scale the K-value could display variations due to changes in the sediment properties.

Initial volumes of inlet morphologic elements were set to zero at both inlets. Although there might have been some sediment in the ebb shoal complex at Indian River Inlet before it was stabilized, it was assumed that this amount was negligible in comparison with the growth occurring after stabilization. The equilibrium volumes for Ocean City Inlet were based on the

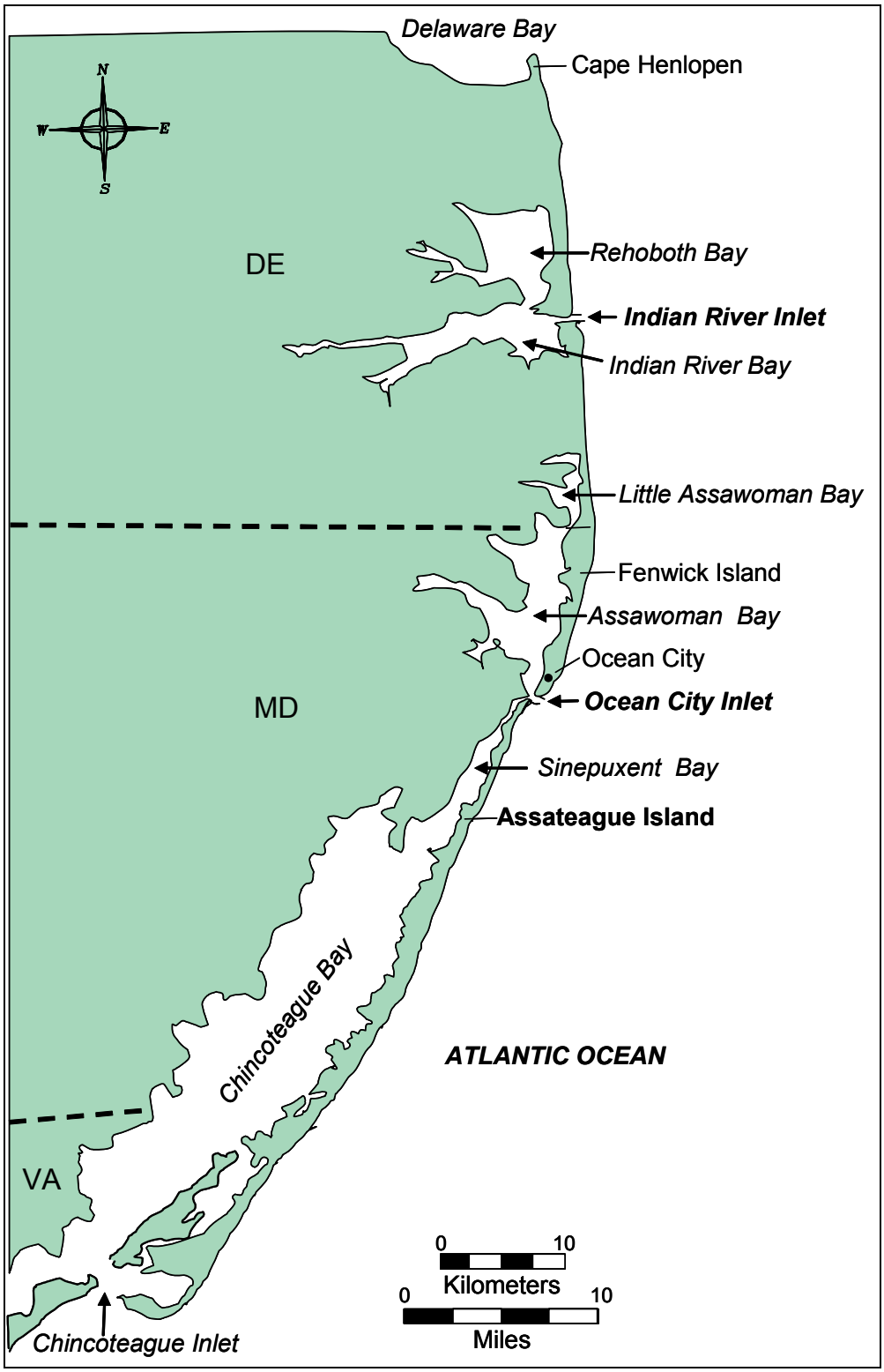

Figure 8. Location map for Delmarva Peninsula

estimates presented by Kraus (2000). For Indian River Inlet, the relationship by Walton and Adams (1976) was applied in combination with data presented in Lanan and Dalrymple (1977) and Perlin et al. (1983). The equilibrium volume of the ebb shoal complex at Ocean City Inlet was 10 million m^3 and at Indian River Inlet 7 million m^3. Partitioning of this volume between the different morphological elements was made as for the Long Island simulations.

Transport by overwash is significant part of the sediment budget along the northern part of Assateague Island (Leatherman 1976). Overwash was included in Cascade as a sink term in the sediment volume conservation equation having a strength that varied in space. The hypothesis was that the material pushed shoreward as overwash would not alter the cross-sectional profile shape and mainly translate the profile onshore. Observed shoreline recession from 1850 to 1933, before Ocean City Inlet opened, was converted to an equivalent cross-shore sediment transport rate. It was assumed, in accordance with Everts (1983, 1985) that most of this recession was caused by overwash. A sink term with a linearly varying strength was added in Cascade based on the observed recession. Because the stretch of coast exposed to overwash has a typical maximum (dune) elevation that is lower than the other part of the coastline, the depth of closure was reduced in this area (compare Rosati and Ebersole 1996). The height of the active profile was set at D_T = 8 m (from the berm to the ocean bottom), except in the overwash area where it was set to 6 m.

Changes in jetty lengths were not modeled, but held constant during the simulation period. Also, an empirical coefficient was introduced in the bypassing algorithm to improve the simulation and to take into account that the employed shoreline corresponded to the high-water shoreline and not the mean water level shoreline. A constant factor of 0.75 was applied to the bypassing ratio computed with Equation 14. Sources and sinks incorporated in the simulation besides the overwash transport were: beach nourishment north of Indian River Inlet (Lanan and Dalrymple 1977) and sediment transport through the south jetty at Ocean City Inlet (Dean and Perlin 1977). All sources and sinks were given a constant strength in time and space during the period they were employed.

Annual net longshore transport rate. Figure 9 plots the spatial variation in the mean annual net longshore sediment transport rate Q_{net} from Cape Henlopen to Chincoteague Inlet calculated by Cascade for the time period 1933-1980 (transport to the north is negative). The computed rates agree well with reported values: Q_{net} = 130,000 m^3/year (to the north) south of Indian River Inlet (Lanan and Dalrymple 1977), Q_{net} = 130,000 m^3/year (to the south) north of Ocean City Inlet (Dean and Perlin 1977), and Q_{net} = 350,000 m^3/year (to the north) at Cape Henlopen (Duane et al. 1972). Also, Cascade reproduces the divergent nodal region in longshore transport known to be located between Indian River Inlet and Ocean City Inlet (Mann and Dalrymple 1986). The model produces another reversal in the longshore transport about 30 km south of Ocean City Inlet that has not been confirmed by observation presented in the literature. Because of the spit growth at Chincoteague, it may be argued that the transport is mainly to the south. However, even though the spit is growing, the long-term net transport could still be to the north. Further investigation is needed to clarify this issue.

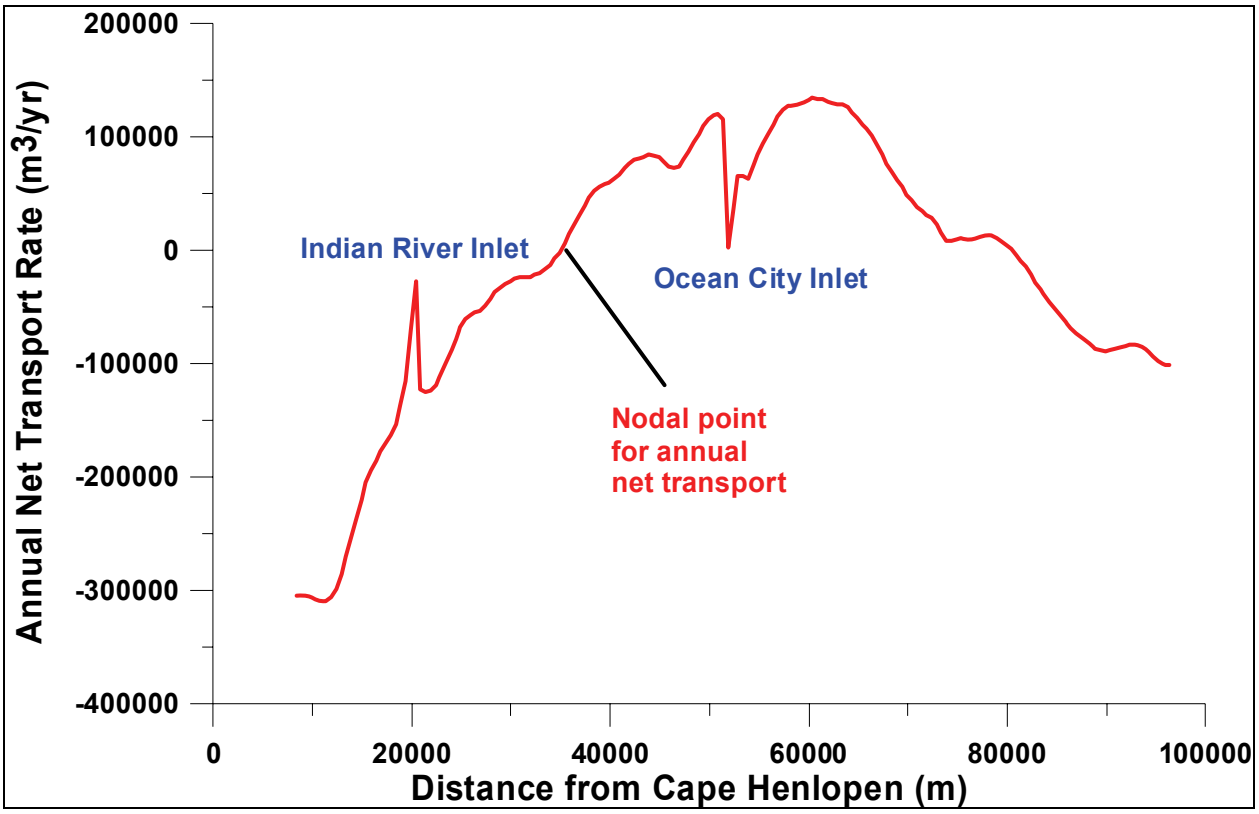

Figure 9. Calculated average net annual longshore sediment transport rate along Delmarva Peninsula based on a simulation from 1933 to 1980

Coastal evolution in connection with inlet opening. Figure 10 displays the calculated and measured shoreline evolution from 1933 to 1980 (the two shorelines fall on top of each other at the scale of the figure). The significant erosion that has occurred downdrift of Ocean City Inlet due to sediment trapping by the north jetty and growth of the ebb shoal complex, as well as by overwash transport, is reproduced. Updrift sediment trapping induces at seaward advance of the shoreline at the northern jetty. The ebb shoal at Indian River Inlet also causes erosion downdrift the inlet, although the shoreline orientation makes it difficult to appreciate the magnitude.

Figure 10 illustrates that Cascade maintains overall regional shoreline shape in agreement with observations. The evolution of the shoreline at the local scale takes place with respect to the regional shoreline orientation, which ensures that the shoreline features at the regional scale is preserved, but makes it necessary to specify this orientation. In this study, the regional shoreline orientation was obtained from the filtered 1933 shoreline measured prior to the inlet opening. A spatial window of about 7 km was employed for the filtering based on experience gained in the Long Island study.

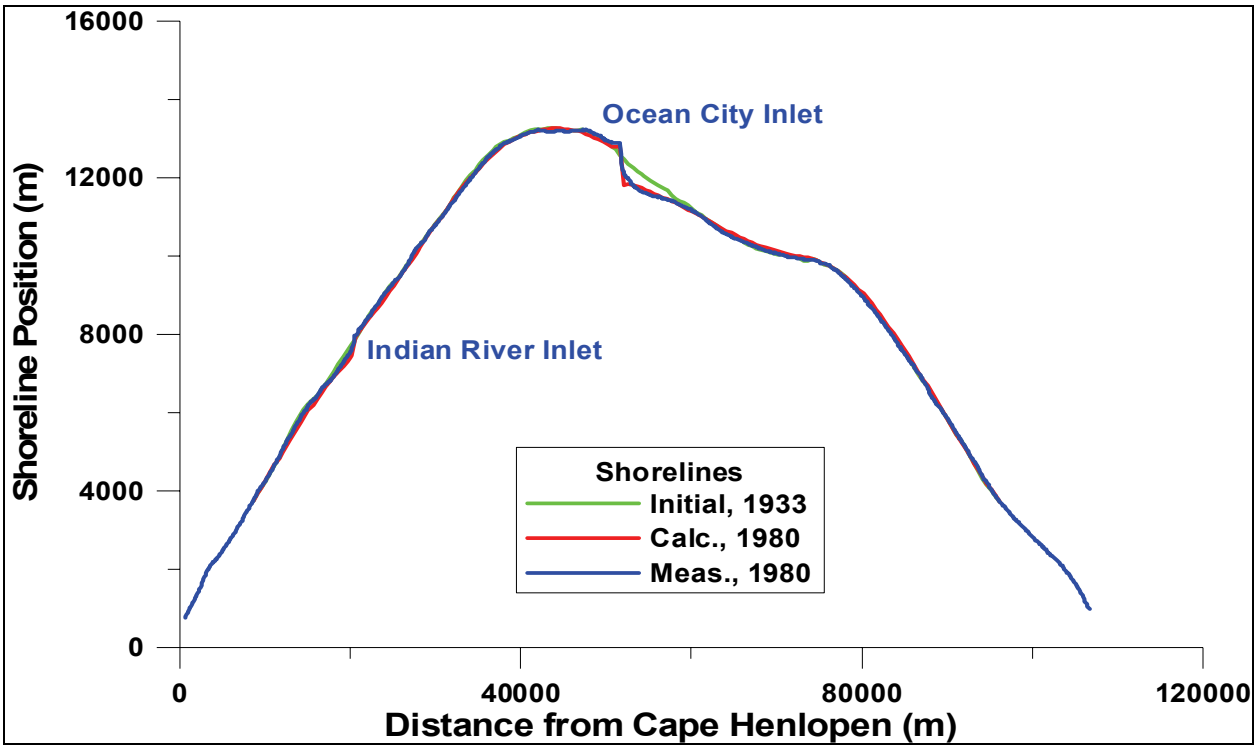

Figure 10. Calculated and measured shoreline evolution along Delmarva Peninsula, 1933 to 1980

To more clearly reveal the shoreline response, Figure 11 compares the calculated and measured change in shoreline position with respect to the 1933 shoreline. The calculations reproduce trends in shoreline advance and recession updrift and downdrift, respectively, of Ocean City Inlet. Total eroded volume downdrift the inlet is also satisfactorily predicted, whereas the total amount of updrift accumulation is less well estimated. The calculations show significant recession updrift the inlet that is not supported by the measurements. Possibly, some beach nourishments have been carried out in this area that may explain the discrepancy. Everts (1985) stated that close to 1 million m^3 of material was put on the Ocean City beaches north of the inlet in 1962. Other sources did not confirm this, however, so no material was added in this area during the simulation.

The calculated evolution around Indian River Inlet deviates more from the observed evolution, although the main features of the response are still obtained. Several of the trends in shoreline evolution are also predicted by Cascade, which is encouraging and indirectly supports the general model performance as well as the input conditions. Further south of Ocean City Inlet, the model calculations show some accumulation, whereas the observations indicate slight erosion. One explanation for the difference may be overwash transport, which was not included for this area because no documentation on overwash prior to inlet opening was available to this study. For large regional stretches and long time periods, it is clear that overwash and breaching must be represented in coastal evolution models such as Cascade.

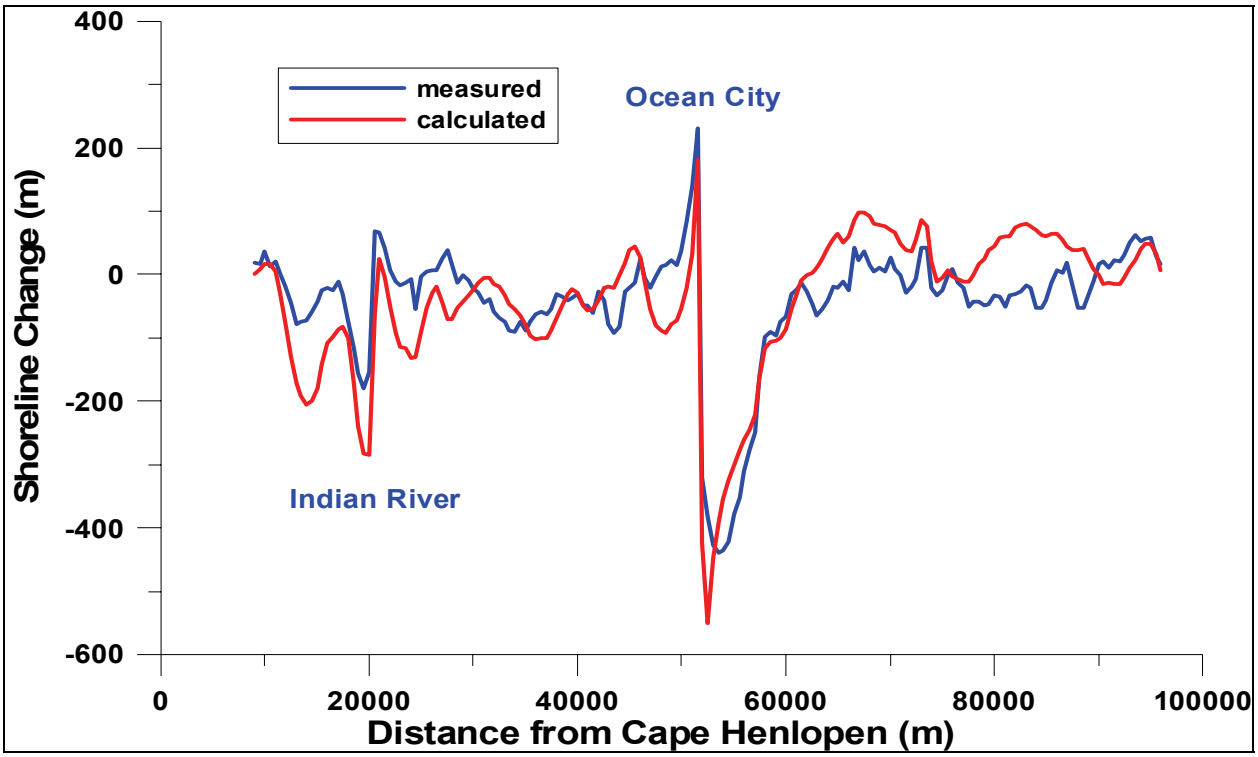

Figure 11. Calculated and measured shoreline change along Delmarva Peninsula, 1933 to 1980

Ebb shoal development. Limited measurements were available for comparison with the calculated volumes of the morphological elements at the inlets. For Indian River Inlet only the total volume of the ebb shoal and bypassing bars at selected times was available (Lanan and Dalrymple 1977; Perlin et al. 1983), and Kraus (2000) presented individual values for the ebb shoal, bypassing bar, and attachment bar volumes for Ocean City Inlet. Figures 12a and 12b show comparisons between the calculated and measured ebb shoal and bypassing bar volumes at Ocean City and Indian River Inlet, respectively. The calculations for Ocean City display marked underestimation, which is due to the excessively slow filling of the downdrift bypassing bar. An increase in the net transport rate through a larger K-value could remedy this and may be related to underestimation in wave input. Figure 12a shows that there are periods with strong growth in the ebb shoal-bypassing bar followed by periods with modest development. To accurately simulate the shoal evolution, the actual wave forcing and its sequence should be known. This was not the case in the present simulation, because only waves from the 1976-1995 hindcast were available. One possibility for arriving at more representative calculation results would be by Monte-Carlo simulation with the wave input randomly selected from the representative wave time series. Such simulations would generate a family of predictions that could be statistically analyzed to provide a mean together with range estimates.

The calculated ebb shoal-bypassing bar growth at Indian River Inlet shows better agreement with the measurements, except at the very beginning. Initially, the growth is too rapid, which is a result of simplified modeling of the inlet boundary condition. In the present simulation, it was assumed that the equilibrium volumes for the morphological elements were those corresponding to the tidal prisms for the inlet after the jetties were installed in 1938-39. Because this assumption should lead to an overestimation at initial opening, when the inlet was not trained

with structures, the volume growth is too rapid. Cascade has the option to specify varying equilibrium volumes, but no information was available for the present simulation on these volumes prior to inlet stabilization.

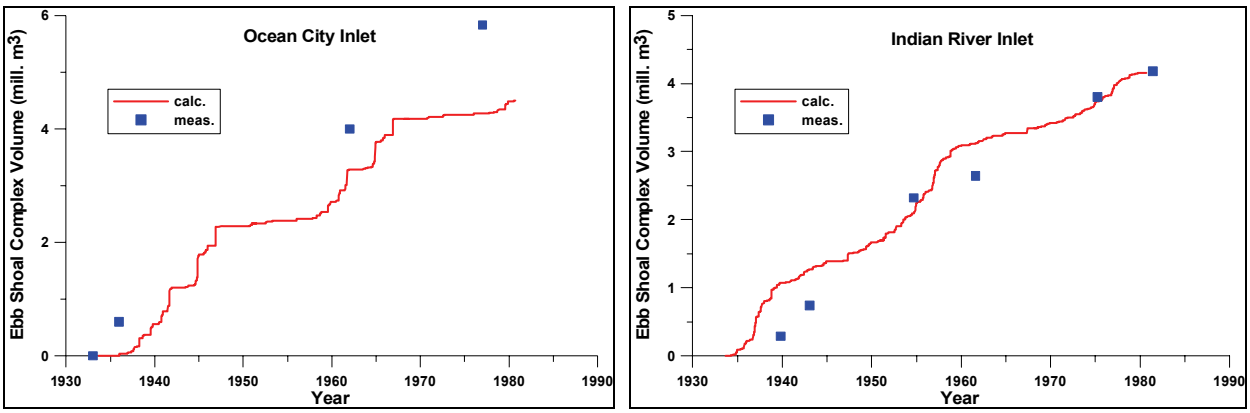

a. Ocean City b. Indian River Inlet

Figure 12. Calculated and measured ebb shoal-bypassing bar evolution between 1933 and 1980

PRODUCT DEVELOPMENT AND AVAILABILITY: Cascade is available to both U.S. Army Corps of Engineers (USACE) and non-USACE interested parties. For USACE employees, Cascade can be obtained by emailing to "SMS" in the Global Address Book. For non-Corps parties, please contact EMS-I at sales@ems-i.com.

ADDITIONAL INFORMATION: This technical note was prepared by Dr. Magnus Larson, professor, Department of Water Resources Engineering, Lund University, and by Dr. Nicholas C. Kraus, senior scientist, and Mr. Kenneth J. Connell, research physical scientist, Coastal and Hydraulics Laboratory, U.S. Army Engineer Research and Development Center. The study was conducted as an activity of the Coastal Morphology Modeling and Management (Cascade) work unit of the System-Wide Water Resources Program (SWWRP). For information on SWWRP, please consult https://swwrp.usace.army.mil/ or contact the Program Manager, Dr. Steven L. Ashby at Steven.L.Ashby@erdc.usace.army.mil. Questions about this technical note may be addressed to Mr. Connell at (601-634-2840; Kenneth.J.Connell@erdc.usace.army.mil). This technical note should be cited as follows:

> Larson, M., N. C. Kraus, and K. J. Connell. (2006). *Cascade Version 1: Theory and model formulation.* ERDC TN-SWWRP-06-7, U.S. Army Engineer Research and Development Center, Vicksburg, MS. https://swwrp.usace.army.mil/

REFERENCES

Anders, F. J. and M. Hansen. 1990. *Beach and borrow site sediment investigation for a beach nourishment at Ocean City, Maryland.* Technical Report CERC-90-5. Vicksburg, MS: Coastal Engineering Research Center, U.S. Army Engineer Waterways Experiment Station.

Anders, F. J., S. G. Underwood, and S. M. Kimball. 1987. Beach and nearshore sediment sampling on a developed barrier, Fenwick Island, Maryland. *Proceedings Coastal Sediments '87*, ASCE, 1,732-1,744.

Bayram, A., M. Larson, and H. Hanson. In preparation. A new formula for the total longshore sediment transport rate. *Coastal Engineering*.

Bocamazo, L. M., and W. G. Grosskopf. 1999. Beach response to groins, Westhampton, New York. *Proceedings Coastal Sediments 99*, ASCE, 2,073-2,089.

Connell, K. J., and N. C. Kraus. 2006. *Cascade Version 1: User's guide.* ERDC TN-SWWRP-06-x. Vicksburg, MS: U.S. Army Engineer Research and Development Center. https://swwrp.usace.army.mil/

Czerniak, M. T. 1977. Inlet interaction and stability theory verification. *Proceedings Coastal Sediments '77*, ASCE, 754-773.

Dean, R. G. 1977. *Equilibrium beach profiles: U.S. Atlantic and Gulf Coasts.* Department of Civil Engineering, Ocean Engineering Report No. 12. Newark, DE: University of Delaware.

Dean, R. G. 1991. Equilibrium beach profiles: Characteristics and applications. *Journal of Coastal Research* 7(1), 53-84.

Dean, R. G., and M. Perlin. 1977. Coastal engineering study of Ocean City Inlet, Maryland. *Proceedings Coastal Sediments '77*, ASCE, 520-542.

Duane, D. B., M. E. Field, E. P. Meisburger, D. J. P. Swift, and S. J. Williams. 1972. Linear shoals on the Atlantic inner continental shelf, Florida to Long Island. In *Shelf Sediment Transport*, 447-498, ed. Swift, Duane, and Pilkey, Dowden, Stroudsburg, PA : Hutchinson&Ross, Inc.

Everts, C. H. 1983. Shoreline changes downdrift of a littoral barrier. *Proceedings Coastal Structures '83*, ASCE, 673-689.

Everts, C. H. 1985. Effect of sea level rise and net sand volume change on shoreline position at Ocean City, Maryland. In *Potential impacts of sea level rise on the beach at Ocean City, Maryland,* EPA 230-10-85-013, U.S. Environmental Protection Agency, Washington DC.

Gebert, J. A., K. D. Watson, and A. T. Rambo. 1992. 57 years of coastal engineering practice at a problem inlet: Indian River Inlet, Delaware. *Proceedings Coastal Engineering Practice '92*, ASCE, 503-519.

Hanson, H., M. Larson, and M. B. Gravens. (in preparation). New algorithm for the total longshore sand transport rate forced by waves and currents. *Coastal Engineering*.

Headquarters, U. S. Army Corps of Engineers. 2001. *Coastal Engineering Manual*, Part 3-2, *Coastal Sediment Processes.* EM 1110-2-1100, Washington, DC.

Kana, T. W. 1995. A mesoscale sediment budget for Long Island, New York. *Marine Geology* 126, 87-110.

Kraus, N. C. 2000. Reservoir model of ebb-tidal shoal evolution and sand bypassing. *Journal of Waterway, Port, Coastal, and Ocean Engineering* 126(6), 305-313.

Kraus, N. C. 2006. Coastal inlet functional design: Anticipating morphologic response. *Proceedings Coastal Dynamics '05*, ASCE.

Kraus, N. C., H. Hanson, and S. Blomgren. 1994. Modern functional design of groins. *Proceedings 24th Coastal Engineering Conference*, ASCE, 1,327-1,342.

Kraus, N. C. and M. Larson. 1991. *NMLONG: Numerical model for simulating the longshore current. Report 1. Model development and tests.* Technical Report DRP-91-1, Vicksburg, MS: Coastal Engineering Research Center, U.S. Army Engineer Waterways Experiment Station.

Kriebel, D. L., N. C. Kraus and M. Larson. 1991. Engineering methods for predicting beach profile response.*Proceedigs Coastal Sediments '91*, ASCE, 557-571.

Lanan, G. A., and R. A. Dalrymple. 1977. *A coastal engineering study of Indian River, Delaware.* Ocean Engineering Technical Report 14, Newark, DE: Department of Civil Engineering, University of Delaware.

Larson, M. 1995. Model for decay of random waves in the surf zone. *Journal of Waterway, Port, Coastal and Ocean Engineering*, 121(1), 1-12.

Larson, M., and H. Hanson. 1996. Schematized numerical model of three-dimensional beach change. *Proceedings 10th Congress of the Asia and Pacific Division*, 325-332, Langkawi, Malaysia: IAHR.

Larson, M., and N. C. Kraus. 2003. Modeling regional sediment transport and coastal evolution along the Delmarva Peninsula. *Proceedings Coastal Sediments '03*, ASCE (on CD).

Larson, M., and A. Bayram. 2005. Calculating cross-shore distribution of longshore sediment transport. In *Port and Coastal Engineering. Developments of Science and Technology*, ed. Per Bruun, Special Issue No. 46, *Journal of Coastal Research*, 203-235.

Larson, M., H. Hanson, and N. C. Kraus. 1987. *Analytical solutions of the one-line model of shoreline change.* Technical Report CERC 87-15, Vicksburg, MS: Coastal Engineering Research Center, U.S. Army Engineer Waterways Experiment Station.

Larson, M., J. D. Rosati, and N. C. Kraus.. 2002a. *Overview of regional coastal processes and controls.* Coastal and Hydraulics Engineering Technical Note CHETN XIV-4, Vicksburg, MS: U.S. Army Engineer Research and Development Center. http://chl.wes.army.mil/library/publications/chetn/pdf/chetn-xiv4.pdf

Larson, M., N. C. Kraus, and H. Hanson. 2002b. Simulation of regional longshore sediment transport and coastal evolution – The Cascade model. *Proceedings 28th Coastal Engineering Conference*, World Scientific Press, 2,612-2,624.

Leatherman, S. P. 1976. Barrier island dynamics: Overwash processes and aeolian transport. *Proceedings 15th Coastal Engineering Conference*, ASCE, 1,958-1,974.

Mann, D. W. and W. A. Dalrymple. 1986. A quantitative approach to Delaware's nodal point. *Shore and Beach* 54(2), 13-16.

Morang, A. 1999. *Shinnecock Inlet, New York, Site investigation, Report 1: Morphology and historical behavior.* Technical Report CHL-98-32, U.S. Army Corps of Engineers, Waterways Experiment Station, Vicksburg, MS.

Nersesian, G. K., N. C. Kraus, and F. C. Carson. 1992. Functioning of groins at Westhampton Beach, Long Island, New York. *Proceedings 23rd Coastal Engineering Conference*, ASCE, 3,357-3,370.

Panuzio, F. L. 1968. The Atlantic coast of Long Island. *Proceedings 11th Conference on Coastal Engineering*, ASCE, 1,222-1,241.

Perlin, M., B. Y. H. Chen, R. A. Dalrymple, R. G. Dean, and J. C. Kraft. 1983. *Sediment budget and sand bypassing system parameters for Delaware's Atlantic Coast.* Unpublished report, Coastal and Offshore Engineering and Research, Inc., Newark, DE.

Ramsey, K. W. 1999. *Beach sand textures from the Atlantic coast of Delaware.* Open File Report No. 41, Delaware Geological Society, Delaware.

Rosati, J. D., and B. A. Ebersole. 1996. Littoral impact of Ocean City Inlet, Maryland, USA. *Proceedings 25th Coastal Engineering Conference*, ASCE, 2,779-2,792.

Rosati, J. D., M. B. Gravens, and W.G. Smith. 1999. Regional sediment budget for Fire Island to Montauk Point, New York, USA. *Proceedings Coastal Sediments '99*, ASCE, 802-817.

Shore Protection Manual. 1984. 4th ed, 2 Vol, U.S. Army Engineer Waterways Experiment Station. Washington, DC: U.S. Government Printing Office.

Stauble, D. K., A. W. Garcia, N. C. Kraus, W. G. Grosskopf, and G. P. Bass. 1993. *Beach nourishment project response and design evaluation: Ocean City Maryland.* Technical Report CERC-93-13, Vicksburg, MS: Coastal Engineering Research Center, U.S. Army Engineer Waterways Experiment Station.

Walton, T. L., and W. D. Adams. 1976. Capacity of inlet outer bars to store sand. *Proceedings 15th Coastal Engineering Conference*, ASCE, 1919-1937.